CHINESE OPTICS LETTERS

Vol. 19, No. 10 | October 2021

Photonic-assisted FSK signal generation based on carrier phase-shifted double sideband modulation

Muguang Wang (王目光)[1*], Yu Tang (唐 宇)[1], Jian Sun (孙 剑)[2], Jing Zhang (张 静)[1], Qi Ding (丁 琪)[1], Beilei Wu (武蓓蕾)[1], and Fengping Yan (延凤平)[1]

[1] Key Laboratory of All Optical Network and Advanced Telecommunication Network, Ministry of Education, Institute of Lightwave Technology, Beijing Jiaotong University, Beijing 100044, China

[2] School of Information and Communication Engineering, Beijing Information Science and Technology University, Beijing 100101, China

*Corresponding author: mgwang@bjtu.edu.cn

Received January 27, 2021 | Accepted March 18, 2021 | Posted Online August 18, 2021

An approach to generate high-speed and wideband frequency shift keying (FSK) signals based on carrier phase-shifted double sideband (CPS-DSB) modulation is proposed and experimentally validated. The core part of the scheme is a pair of cascaded polarization-sensitive $LiNbO_3$ Mach–Zehnder modulators and phase modulators, whose polarization directions of the principal axes are mutually orthogonal to each other. A proof-of-concept experiment is carried out, where a 0.5 Gb/s FSK signal with the carrier frequencies of 4 and 8 GHz and a 1 Gb/s FSK signal with the carrier frequencies of 8 and 16 GHz are generated successfully.

Keywords: microwave photonics; frequency shift keying; polarization-sensitive modulator; microwave signals generation; carrier phase-shifted double sideband modulation.

DOI: 10.3788/COL202119.103901

1. Introduction

Traditionally, microwave signals generated in the electrical domain by electronic devices have limited bandwidth and tunability, owing to the electronic bottleneck. Having the intrinsic advantages of broadband, reconfigurability, low system complexity, and immunity to electromagnet interference, microwave photonics has attracted more and more research interests in radar systems[1,2], sensing and measurement fields[3,4], and radio over fiber (RoF) systems[5,6]. Modulation formats including phase shift keying (PSK)[1], amplitude shift keying (ASK)[7], and frequency shift keying (FSK)[8–12] and higher modulation formats such as quadrature amplitude modulation (QAM)[13] have been investigated by photonic-assisted techniques. Among them, FSK signals are widely used in various communication systems and radar systems[14] due to their good noise and attenuation immunity[15].

A binary FSK signal is represented in terms of two frequencies. The frequency carrying bit '1' is called the mark frequency, and the other frequency carrying bit '0' is designated the space frequency. How to switch between the mark frequency and the space frequency is a key technique for FSK signal generation. Cao *et al.* reported an FSK signal generation scheme by switching the bias point of a Mach–Zehnder modulator (MZM)[8]. The MZM was biased either at the quadrature transmission point (QTP) or null transmission point (NTP) driven by an electrical signal with different radio frequency (RF) amplitudes and direct current (DC) components for bit '0' and bit '1'. In Ref. [9], a scheme for FSK signal generation by switching the bias of a dual-drive MZM (DDMZM) has been demonstrated. By properly selecting the operation bandwidth of an antenna, a microwave FSK signal can be sent into free space, while the non-ignorable higher-order-frequency components are filtered out. Ye *et al.* utilized the set of an MZM, a polarization modulator (PolM), and a polarization-maintaining fiber Bragg grating (PM-FBG) to generate an FSK signal with tunable carrier frequency[10]. The PolM and PM-FBG can transform the signal to a wavelength shift keying one. However, the wavelength-dependent PM-FBG may reduce the flexibility of the whole system, and the beat of incoherent optical signals may degrade the quality of the FSK signal. Huang *et al.* used a cascaded PolM and dual-polarization MZM to generate FSK signals[11]. A polarization shift keying signal was generated by properly modulating PolM with an on–off keying (OOK) signal, and then optical signals in the two orthogonal directions are driven by two microwave signals with different frequencies. In Ref. [12], an equivalent photonic switch for microwave FSK signal generation based on a polarization-multiplexing DDMZM (PM-DDMZM) has been reported. One sub-DDMZM was driven by a binary data sequence and an RF signal, and the other DDMZM was driven by an inverse data sequence and another RF signal.

The two DDMZMs work cooperatively and combine the two orthogonal polarized optical signals to generate an FSK signal. The proposed FSK signal generator takes the advantages of simple structure and low loss, but two data sequences, including the original data sequence and the inverse data sequence, have to be used.

In this Letter, we propose and experimentally demonstrate a photonic-assisted approach for FSK signal generation based on specially designed carrier phase-shifted double sideband (CPS-DSB) modulation. The joint operation of the polarization-sensitive MZM and phase modulator (PM) helps to realize the switch between mark frequency and space frequency by introducing different phase shifts between the optical carrier (OC) and the ±1st-order sidebands along the two orthogonal axes of the PM. By adjusting the driven RF signals of the MZM and PM, a microwave FSK signal is generated at the output of the photodiode (PD). A theoretical analysis is presented and verified by a proof-of-concept experiment. A 0.5 Gb/s FSK signal with the carrier frequencies of 4 and 8 GHz and a 1 Gb/s FSK signal with the carrier frequencies of 8 and 16 GHz are generated successfully. The electrical spectra, waveforms, and eye diagrams of the FSK signals are investigated.

2. Principle

The proposed schematic diagram for FSK signal generation based on the photonic-assisted CPS-DSB technique is shown in Fig. 1(a), and the spectral evolution of the polarized light wave at different positions is also depicted in Fig. 1(b). The polarization direction of the linearly polarized continuous-wave (CW) light wave emitted from a laser diode (LD) is adjusted to have an angle of α to the principal axis of the polarization-sensitive MZM (parallel to the X axis) by a polarization controller (PC_1). The optical field of the light wave in the two orthogonal directions can be written as

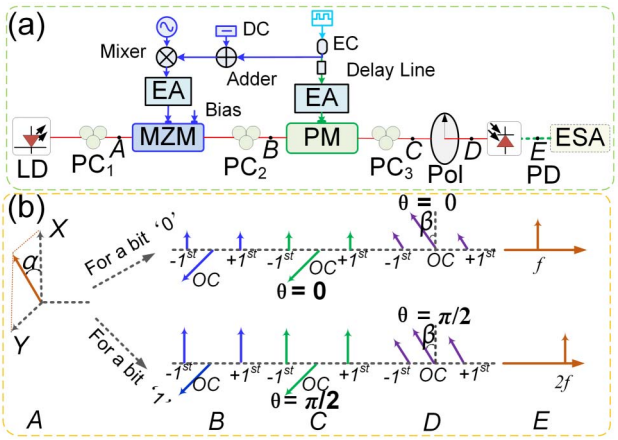

Fig. 1. (a) Proposed schematic diagram for FSK signal generation based on CPS-DSB modulation. (b) Spectral evolution of the injected CW light wave at different positions in the system.

$$\begin{bmatrix} E_x \\ E_y \end{bmatrix} = E_0 \cdot e^{j\omega_0 t} \times \begin{bmatrix} \cos\alpha \\ \sin\alpha \end{bmatrix}, \tag{1}$$

where E_0 and ω_0 are the amplitude and angular velocity of the CW light wave. The key devices of the CPS-DSB system are the polarization-sensitive $LiNbO_3$ MZM and PM. The modulation efficiency of the $LiNbO_3$ crystal in the direction of the externally applied electric field, i.e., the principal axis of the crystal, is much larger than that in the orthogonal direction due to the polarization-dependent electro-optical property of the $LiNbO_3$ crystal[16]. The MZM is biased at the NTP to generate a special orthogonal double sideband (O-DSB) modulated signal, where the polarization direction of the OC is orthogonal to that of the sidebands. In the principal direction, the light wave is with carrier-suppressed intensity modulated with a large modulation index (MI) and generates obvious double sidebands, while, in the orthogonal direction, the signal is hardly modulated, and the orthogonal OC E_y passes through the MZM directly without modulation. The corresponding optical spectra are depicted in Fig. 1(b) at position B in the system.

When a microwave signal $S(t) = V_m \cos(\omega_m t)$ is applied on the MZM, the optical field of the light wave at the output of the MZM can be expressed as

$$\begin{bmatrix} E_x \\ E_y \end{bmatrix} = E_0 \cdot e^{j\omega_0 t} \times \begin{bmatrix} \cos\alpha \cos[\gamma \cos(\omega_m t) + \pi/2] \\ \sin\alpha \end{bmatrix}, \tag{2}$$

where V_m and ω_m are the amplitude and angular frequency of the microwave signal, respectively, and $\gamma = \pi V_m/(2V_{\pi\mathrm{MZM}})$ is the MI ($V_{\pi\mathrm{MZM}}$ is the half-wave voltage of the MZM). Then, the special O-DSB modulated signal is led into a PM via PC_2 to make the orthogonal OC aligned with the principal axis of the PM (parallel to the Y axis). The PM can introduce different phase shifts to the light waves in the two orthogonal axes of the PM depending on the amplitude of the driven signal in the RF port[17]. The signal at the output of the PM can be expressed as

$$\begin{bmatrix} E_x \\ E_y \end{bmatrix} = E_0 \cdot e^{j\omega_0 t} \times \begin{bmatrix} \cos\alpha \cos[\gamma \cos(\omega_m t) + \pi/2] \\ \sin\alpha \exp(j\theta) \end{bmatrix}, \tag{3}$$

where θ is the phase shift caused by the PM. Strictly speaking, if the modulation in the orthogonal axis is considered, 0 and $\pi/2$ phase shifts between the two orthogonal polarization directions should be introduced in our approach. Considering that the modulation efficiency in the orthogonal axis direction is much smaller than that in the principal axis direction, the amplitudes of bit '0' and bit '1' of the driven binary signal are simply set to be 0 and $V_{\pi\mathrm{PM}}/2$, respectively, where $V_{\pi\mathrm{PM}}$ is the half-wave voltage of the PM. Therefore, either a 0 or $\pi/2$ phase shift is introduced between the orthogonal OC and the ±1st-order sidebands. Then, the two orthogonal polarized components of the signal interfere at a polarizer (Pol). The polarization direction of phase modulated OC has an angle of β to the principal direction of the Pol. Thus, the amplitude of the optical signal at the output of the Pol can be written as

$$E = E_0 \cdot e^{j\omega_0 t} \times \{\cos\alpha \cos\beta \cos[\gamma \cos(\omega t) + \pi/2] + \sin\alpha \sin\beta \exp(j\theta)\}. \quad (4)$$

Considering the small signal modulation condition and the bias point of the MZM, only the OC and the ±1st-order sidebands are taken into account. Then, the optical field received by the PD can be rewritten as

$$E = E_0 \cdot e^{j\omega_0 t} \times [\cos\alpha \cos\beta \cdot J_1(\gamma) \cdot (e^{j\omega_m t} + e^{-j\omega_m t}) + \sin\alpha \sin\beta \exp(j\theta)], \quad (5)$$

where J_1 is the first-order Bessel function of the first kind. Obviously, as can be seen from Eqs. (4) and (5), a CPS-DSB modulated signal is achieved.

Then, optical-to-electrical conversion is performed in the PD. Ignoring the DC component, the electrical current can be expressed as

$$i \propto E \cdot E^{*} \propto E_0^2[J_1(\gamma)^2 \cos^2\alpha \cos^2\beta \cos(2\omega_m t) + 2J_1(\gamma) \sin\alpha \sin\beta \cos\alpha \cos\beta \cos(\omega_m t) \cos\theta]. \quad (6)$$

To optimize the amplitude of the electrical current, let $\alpha = \pi/4$, $\beta = \pi/4$ for simplicity. The generated electrical signal can be rewritten as

$$i \propto E_0^2[J_1(\gamma)^2 \cos(2\omega_m t) + 2J_1(\gamma) \cos(\omega_m t) \cos\theta]. \quad (7)$$

Recall that θ is the phase shift induced by the PM. For a bit '0', θ equals zero, and the electrical signal is presented as

$$i_0 \propto E_0^2[J_1(\gamma_0)^2 \cos(2\omega_m t) + 2J_1(\gamma_0) \cos(\omega_m t)], \quad (8)$$

where γ_0 is the MI for a bit '0'. Although there are both fundamental-frequency components and frequency-doubled components in the expression, the frequency-doubled component can be neglected, and the fundamental-frequency component is the dominant one by choosing an appropriate γ_0. While for a bit '1', θ equals $\pi/2$, and the electrical signal is presented as

$$i_1 \propto E_0^2 J_1(\gamma_1)^2 \cos(2\omega_m t), \quad (9)$$

where γ_1 is the MI for bit '1'. As can be seen, a frequency-doubled signal is generated.

The above operation principle can also be explained by analyzing the relationship of the beat signals between different optical-frequency components of the modulated signal. As shown in Fig. 1(b) at position *C*, for a bit '0', the beat signal between the −1st sideband and the OC and the beat signal between the OC and the +1st sideband are in phase, and therefore a constructive interference occurs. An equivalent intensity modulation as well as a dominant fundamental-frequency component is generated. Whereas for a bit '1', a phase shift of $\pi/2$ is introduced, so the phase difference between the OC and the ±1st-order sidebands is $\pi/2$, and an equivalent phase modulation is formed[18]. Given that the MZM is biased at the NTP, the ±2nd-order and higher-order sidebands are neglected. In the PD following closely the Pol, the beat signal between the −1st sideband and the OC and the beat signal between the OC and the +1st sideband are of reversed phase, leading to destructive interference. Thus, only a frequency-doubled component is generated[19]. The related schematic optical spectra and electrical spectra at positions *D* and *E* are shown in Fig. 1(b). Thus, the switch between the space frequency, i.e., the fundamental frequency and the mark frequency, i.e., the doubled frequency, is realized.

For an FSK signal, the amplitude of the mark-frequency signal and the space-frequency signal should be identical. The amplitude of the sidebands at the output of the MZM needs to be adjustable according to bit '0' and bit '1'. Once the condition

$$A = \begin{cases} A_0 = 2J_1(\gamma_0) \gg J_1(\gamma_0)^2 \\ A_1 = J_1(\gamma_1)^2 \end{cases} \quad (10)$$

is met, the generated microwave FSK signal can be expressed as

$$i \approx \begin{cases} E_0^2 A \cos(\omega_m t) & \text{bit '0'} \\ E_0^2 A \cos(2\omega_m t) & \text{bit '1'} \end{cases}, \quad (11)$$

where A, A_0, A_1 are the amplitude coefficients of the FSK signal, the fundamental component, and the frequency-doubled component, respectively. The values of A_0, A_1 with the change of MI γ are shown in Fig. 2. Here, γ_0 and γ_1 are set to be 0.35 and 1.88, respectively. The amplitude of the data signal fed to the RF port of the MZM is carefully adjusted, as shown in Fig. 1(a). The original unipolar non-return-to-zero (NRZ) data signal generated by a pulse pattern generator is divided into two parts. One part is added by a DC and mixed with a local fundamental-frequency microwave signal to generate an ASK signal. Then, the ASK signal is amplified by an electrical amplifier (EA) to drive the MZM. The other part drives the PM, whose amplitude is also amplified and controlled by an EA. The synchronization between the two branches of signals driving the MZM and the PM is realized by controlling an electrical delay line.

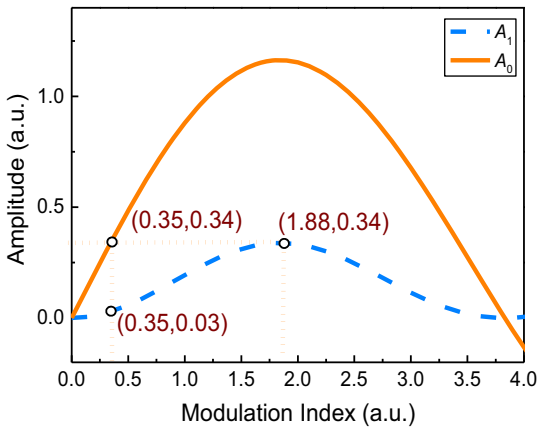

Fig. 2. Values of A_0 and A_1 with the change of MI.

3. Experiment

An experiment generating a 0.5 Gb/s FSK signal with the carrier frequencies of 4 and 8 GHz and a 1 Gb/s FSK signal with the carrier frequencies of 8 and 16 GHz is carried out to verify the performance of the proposed scheme. Firstly, the polarization property of the $LiNbO_3$ crystal is explored. The optical signal emitted from a tunable laser source (TLS, Agilent 8164 A) centered at 1550 nm with a power of 7 dBm is sent to a polarization-sensitive MZM via PC_1. Both the MZM (JDSU) and PM (EOSPACE) are commercially available with 3 dB bandwidths of 10 GHz, and half-wave voltages of 5 V and 3 V, respectively. The optical spectra directly after the MZM biased at NTP driven by an 8 GHz sinusoidal signal are observed by an optical spectrum analyzer (OSA) with a resolution of 0.02 nm, as shown in Fig. 3. Figure 3(a) shows the total spectrum of the special O-DSB modulated signal, and Figs. 3(b) and 3(c) depict the spectra along the orthogonal axis and the principal axis, respectively. As can be seen, the OC in the orthogonal axis is hardly modulated, because the power of the ±1st-order sidebands is 27 dB lower than that of the OC. The case is similar to a polarization-sensitive PM. In the principal axis, the OC is well suppressed, and the power of ±1st-order sidebands is 20 dB higher than that of the OC. In addition, the power of the ±2nd-order sidebands is 27 dB lower compared to the ±1st-order sidebands, so it is reasonable to neglect the ±2nd-order and higher-order sidebands.

To evaluate the performance of the proposed system based on CPS-DSB modulation, an 8 GHz microwave sinusoidal signal and an adjustable DC are applied on the MZM and PM by replacing the two branches of data signals. The insert losses of the $LiNbO_3$ MZM and PM are also polarization sensitive, where the insert loss along the principal axis is about 5 dB less than that along the orthogonal axis. To make the orthogonal OC aligned with the principal axis of the PM, just ensure that the orthogonal OC has the maximum power after passing though the PM by monitoring the optical spectrum at the output of the Pol. Another method to keep the principal axes of the MZM and PM orthogonal to each other is to use a polarization-maintaining fusion splicer to fuse the polarization-maintaining fiber pigtails of the MZM and PM with a polarization rotation of 90°. The PM is driven by the amplitude-adjustable DC acting as binary data sequences of all bit '0' or all bit '1' by adjusting the voltage to be 0 and 1.5 V. Figures 4(a) and 4(c) illustrate the optical spectrum and electrical spectrum, respectively, when the data sequence of all bit '0' is applied. While Figs. 4(b) and 4(d) show the optical and electrical spectra of the all bit '1' case. The electrical spectra are captured by an electrical spectrum analyzer (ESA, Agilent N9010A). The amplitude of the 8 GHz sinusoidal signal of the '0' case and the '1' case is 1.2 V and 6 V, respectively. As can be seen from Figs. 4(a) and 4(b), the MI of the '0' case has a smaller MI compared with the one of the '1' case. In Fig. 4(c), the power of the dominating fundamental-frequency component is 16 dB higher than that of the frequency-doubled component. In Fig. 4(d), the power of the frequency-doubled component is 24 dB higher than that of the fundamental-frequency component as well. It is also shown that the amplitude of the dominant fundamental-frequency component in Fig. 4(c) is almost the same as that of the dominant frequency-doubled component in Fig. 4(d). The above experiment results indicate that by carefully controlling the amplitudes of the RF signals applied on the MZM and the PM, the dominant fundamental-frequency component and the dominant frequency-doubled component can be designated as the space-frequency signal and the mark-frequency signal, respectively.

Afterwards, a 1 Gb/s FSK signal with the carrier frequencies of 8 and 16 GHz is generated. A 1 Gb/s $(2^{31}-1)$ NRZ pseudorandom bit sequence (PRBS) generated by a bit error rate tester (BERT, Agilent N4901B) with an amplitude of 1.1 V is divided into two branches. One branch is added by a 0.2 V DC to generate a unipolar ASK signal, mixed with a 11 dBm 8 GHz microwave carrier, and then enlarged to drive the MZM, while the other is amplified and led to the RF port of the PM to modulate

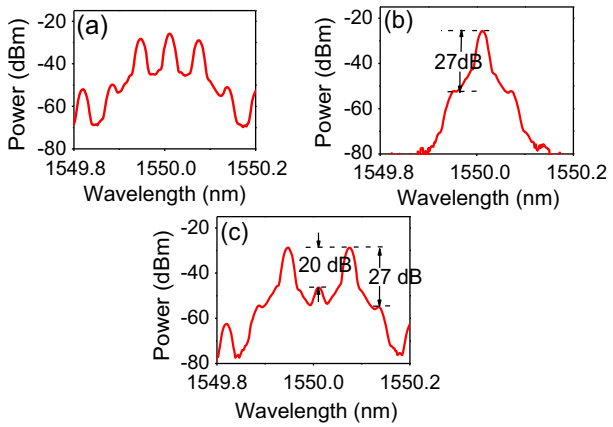

Fig. 3. Optical spectra at the output of the MZM. (a) Total spectrum. (b) Spectrum along the orthogonal axis. (c) Spectrum along the principal axis.

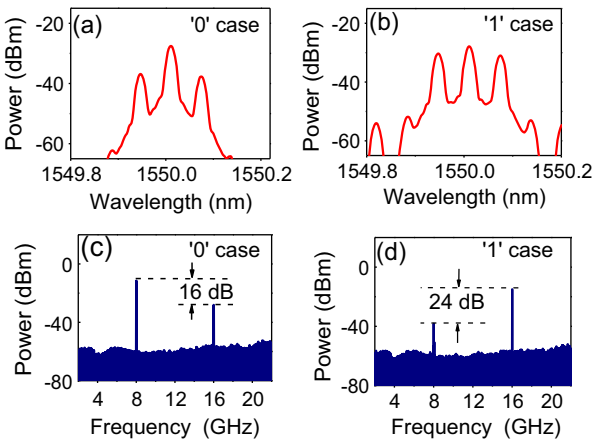

Fig. 4. (a) Optical spectrum and (c) the related electrical spectrum of the '0' case. (b) The optical spectrum and (d) the related electrical spectrum of the '1' case.

the orthogonal OC output from the MZM. An electrical delay line is employed to synchronize the two branches of data signals. After the lights in the two polarization directions interfere with each other in a Pol and are injected into the PD for optical-to-electrical conversion, a microwave FSK signal with the carrier frequencies of 8 and 16 GHz is generated at the output of the PD. The imperfect polarization direction alignment of the devices, imperfect driven signals, as well as low extinction ratio of the Pol would lead to the amplitude imbalance of the mark-frequency and space-frequency signals, the decrease of the extinction ratio of the FSK signal, and finally deteriorate the quality of the FSK signal. Using devices with polarization-maintaining fiber pigtails will reduce the external environment induced polarization fluctuation significantly. The electrical spectrum, waveform, and eye diagram of the FSK signal are captured by an ESA and a high-speed sampling oscilloscope (Agilent, 86100B), as shown in Figs. 5(a)–5(c), respectively. As shown in Fig. 5(a), there are two carrier frequencies at 8 GHz and 16 GHz in the electrical spectrum, among which the 16 GHz carrier is generated by frequency doubling thanks to the CPS-DSB modulation. A piece of temporal waveform carrying a binary data sequence of '01001' in a duration of 5 ns is illustrated in Fig. 5(b). The bit period of the baseband signal is 1 ns. The bits '0' and '1' are carried by the 8 GHz and 16 GHz microwave signals with periods of 125 ps and 62.5 ps, respectively. An eye diagram in a duration of 2 ns is also clearly obtained, as shown in Fig. 5(c).

The photonic-assisted scheme based on CPS-DSB modulation can be considered microwave carrier-frequency and bit-rate independent in the optical domain and can support high-speed and wideband operation when, and only when, the used electrical and optoelectronic devices in the system have enough operation bandwidth. In order to further verify the tunability of frequency and bit rate of the proposal, the generation for a 0.5 Gb/s FSK signal with the carrier frequencies of 4 and 8 GHz is also implemented. The MZM is driven by a 0.5 Gb/s ASK signal at 4 GHz. The electrical spectrum, waveform, and eye diagram of the FSK signal with the carrier frequencies of 4 and

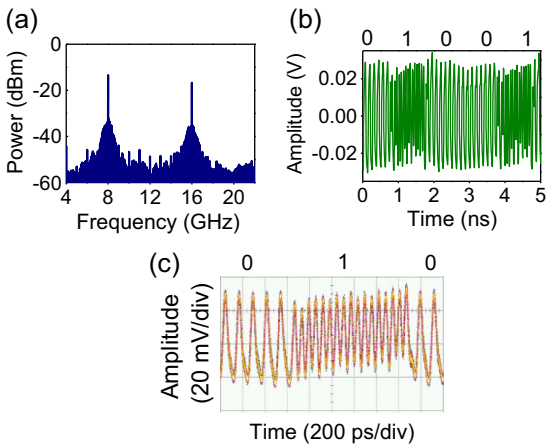

Fig. 5. (a) Electrical spectrum, (b) waveform, and (c) eye diagram of the 1 Gb/s FSK signal with the carrier frequencies of 8 and 16 GHz.

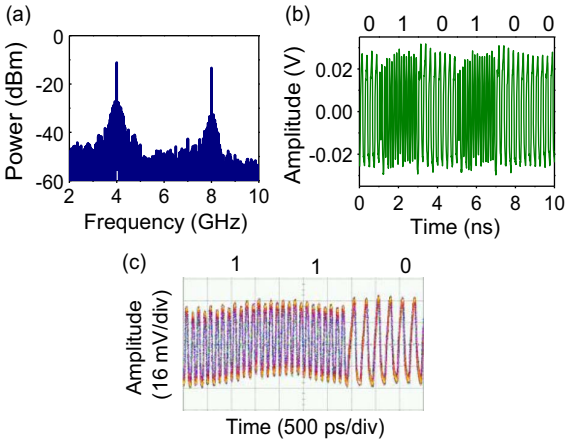

Fig. 6. (a) Electrical spectrum, (b) waveform, and (c) eye diagram of the FSK signal with the carrier frequencies of 4 and 8 GHz.

8 GHz is shown in Figs. 6(a)–6(c). As can be seen, the electrical spectrum, waveform, and eye diagram are clear and clean, which implies a good quality of generated FSK signals. Thus, the wideband operation of the scheme is well verified. The mark-frequency signal is generated by photonic-assisted frequency doubling of the space-frequency signal; therefore, the required bandwidths for the electrical and optical devices are relieved. In addition, in this scheme, the MZM is biased at the NTP, so the ±2nd-order sidebands as well as the OC in the principal axis are suppressed, which will reduce the distortion from ±2nd-order sidebands. Therefore, no additional filter or digital processing is needed.

4. Conclusion

In conclusion, a novel photonic-assisted method for FSK signal generation based on CPS-DSB modulation has been proposed and experimentally validated. By controlling the driven RF signals of the cascaded polarization-sensitive MZM and PM, a high-speed FSK signal with wideband-frequency tunability can be generated. A 0.5 Gb/s FSK signal with carrier frequencies of 4 and 8 GHz and a 1 Gb/s FSK signal with carrier frequencies of 8 and 16 GHz were demonstrated successfully. The proposed scheme is compact and cost effective, supporting high-speed and wideband operation, which may find applications in RoF and radar systems.

Acknowledgement

This work was supported by the National Natural Science Foundation of China (Nos. U2006217, 61775015, 61801017, and 61827818).

References

1. Y. Chen and J. Yao, "Simultaneous multi-frequency phase-coded microwave signal generation at six different frequencies using a DP-BPSK modulator," J. Lightwave Technol. **37**, 2293 (2019).

2. N. Shi, W. Li, N. Zhu, and M. Li, "Optically controlled phase array antenna [Invited]," Chin. Opt. Lett. **17**, 052301 (2019).
3. X. Zou, B. Lu, W. Pan, L. Yan, A. Stöhr, and J. Yao, "Photonics for microwave measurements," Laser Photon. Rev. **10**, 711 (2016).
4. X. Wang, S. Li, X. Jiang, J. Hu, M. Xue, S. Xu, and S. Pan, "High-accuracy optical time delay measurement in fiber link [Invited]," Chin. Opt. Lett. **17**, 060601 (2019).
5. X. Li, J. Yu, and G.-K. Chang, "Photonics-assisted technologies for extreme broadband 5G wireless communications," J. Lightwave Technol. **37**, 2851 (2019).
6. J. Capmany and D. Novak, "Microwave photonics combines two worlds," Nat. Photon. **1**, 319 (2007).
7. K. Tsuji and T. Uehara, "Photonic generation of a phase-switchable ASK signal using orthogonal polarization modes of a single optical phase modulator," in *2017 Opto-Electronics and Communications Conference (OECC) and Photonics Global Conference (PGC)* (2017), p. 1.
8. P. Cao, X. Hu, L. Zhang, J. Wu, X. Jiang, and Y. Su, "Photonic generation of microwave frequency shift keying signal using a single-drive Mach–Zehnder modulator," Opt. Express, **22**, 14433 (2014).
9. Y. Chen, "High-speed and wideband frequency-hopping microwave signal generation via switching the bias point of an optical modulator," IEEE Photon. J. **10**, 2797273 (2018).
10. J. Ye, L. Yan, H. Wang, W. Pan, B. Luo, and X. Zou, "Photonic generation of microwave frequency shift keying signal using a polarization maintaining FBG," IEEE Photon. J. **10**, 2772778 (2018).
11. L. Huang, P. Wang, P. Xiang, D. Chen, Y. Zhang, J. Tao, T. Pu, and X. Chen, "Photonic generation of microwave frequency shift keying signals," IEEE Photon. Technol. Lett. **28**, 1928 (2016).
12. M. Lei, Z. Zheng, C. Song, Y. Bai, J. Qian, S. Huang, and X. Gao, "Equivalent photonic switch for microwave frequency shift keying signal generation," Opt. Lett. **44**, 3138 (2019).
13. J. Zheng, F. Lu, M. Xu, M. Zhu, M. I. Khalil, X. Bao, D. Guidotti, J. Liu, N. Zhu, and G.-K. Chang, "A dual-polarization coherent communication system with simplified optical receiver for UDWDM-PON architecture," Opt. Express **22**, 31735 (2014).
14. N. Levanon and I. I. Cohen, "Binary frequency shift keying for continuous waveform radar," IEEE Trans. Aerosp. Electron. Syst. **53**, 2462 (2017).
15. S.-C. Chan, S.-K. Hwang, and J.-M. Liu, "Radio-over-fiber AM-to-FM upconversion using an optically injected semiconductor laser," Opt. Lett. **31**, 2254 (2006).
16. M. Lawrence, "Lithium niobate integrated optics," Rep. Prog. Phys. **56**, 363 (1993).
17. B. Wu, M. Wang, Y. Tang, J. Sun, and S. Jian, "Photonic microwave signal mixing using sagnac-loop-based modulator and polarization-dependent modulation," IEEE Photon. J. **8**, 5501208 (2016).
18. Y. Shao, X. Han, Q. Ye, B. Zhu, Y. Dai, C. Wang, and M. Zhao, "Low-power RF signal detection using a high-gain tunable OEO based on equivalent phase modulation," J. Lightwave Technol. **37**, 5370 (2019).
19. Y. Qiao, S. Zheng, H. Chi, X. Jin, and X. Zhang, "A frequency-doubling optoelectronic oscillator based on phase modulator," in *2012 IEEE International Topical Meeting on Microwave Photonics* (2012), p. 10.